2017

Impact of Glacial/Interglacial Sea Level Change on the Ocean Nitrogen Cycle

Haojia Ren

Daniel M. Sigman

Alfredo Martínez-García

Robert F. Anderson

Chen Min-Te

See next page for additional authors

Original Publication Citation

Ren, H., Sigman, D. M., Martínez-García, A., Anderson, R. F., Min-Te, C., Ravelo, A. C., . . . Haug, G. H. (2017). Impact of glacial/interglacial sea level change on the ocean nitrogen cycle. *Proceedings of the National Academy of Sciences of the United States of America, 114*(33), E6759-E6766. doi:10.1073/pnas.1701315114

Authors
Haojia Ren, Daniel M. Sigman, Alfredo Martínez-García, Robert F. Anderson, Chen Min-Te, Ana Christina Ravelo, Marietta Straub, George T. F. Wong, and Gerald H. Haug

Impact of glacial/interglacial sea level change on the ocean nitrogen cycle

Haojia Ren[a,1], Daniel M. Sigman[b], Alfredo Martínez-García[c], Robert F. Anderson[d], Min-Te Chen[e], Ana Christina Ravelo[f], Marietta Straub[g], George T. F. Wong[h,i], and Gerald H. Haug[c,j]

[a]Department of Geosciences, National Taiwan University, Taipei 106, Taiwan; [b]Department of Geosciences, Princeton University, Princeton, NJ 08544; [c]Max Planck Institute for Chemistry, 55128 Mainz, Germany; [d]Lamont-Doherty Earth Observatory, Columbia University, Palisades, NY 10964; [e]Institute of Geosciences, National Taiwan Ocean University, Keelung 20224, Taiwan; [f]Ocean Sciences Department, University of California, Santa Cruz, CA 95064; [g]Institute of Radiation Physics, Lausanne University Hospital, 1011 Lausanne, Switzerland; [h]Research Center for Environmental Changes, Academia Sinica, Taipei 11529, Taiwan; [i]Department of Ocean, Earth and Atmospheric Sciences, Old Dominion University, Norfolk, VA 23529; and [j]Department of Earth Sciences, Eidgenössische Technische Hochschule Zürich, 8092 Zurich, Switzerland

Edited by Donald E. Canfield, Institute of Biology and Nordic Center for Earth Evolution, University of Southern Denmark, Odense M., Denmark, and approved July 5, 2017 (received for review January 25, 2017)

The continental shelves are the most biologically dynamic regions of the ocean, and they are extensive worldwide, especially in the western North Pacific. Their area has varied dramatically over the glacial/interglacial cycles of the last million years, but the effects of this variation on ocean biological and chemical processes remain poorly understood. Conversion of nitrate to N_2 by denitrification in sediments accounts for half or more of the removal of biologically available nitrogen ("fixed N") from the ocean. The emergence of continental shelves during ice ages and their flooding during interglacials have been hypothesized to drive changes in sedimentary denitrification. Denitrification leads to the occurrence of phosphorus-bearing, N-depleted surface waters, which encourages N_2 fixation, the dominant N input to the ocean. An 860,000-y record of foraminifera shell-bound N isotopes from the South China Sea indicates that N_2 fixation covaried with sea level. The N_2 fixation changes are best explained as a response to changes in regional excess phosphorus supply due to sea level-driven variations in shallow sediment denitrification associated with the cyclic drowning and emergence of the continental shelves. This hypothesis is consistent with a glacial ocean that hosted globally lower rates of fixed N input and loss and a longer residence time for oceanic fixed N—a "sluggish" ocean N budget during ice ages. In addition, this work provides a clear sign of sea level-driven glacial/interglacial oscillations in biogeochemical fluxes at and near the ocean margins, with implications for coastal organisms and ecosystems.

denitrification | nitrogen fixation | nitrogen isotopes | glacial cycles

Biological productivity in much of the ocean is limited by the supply of biologically available nitrogen ("fixed N") (1). Biological processes are central to the input and output of fixed N to and from the ocean: N_2 fixation by cyanobacteria in surface waters appears to dominate the input of N to the ocean, whereas the main sink is biological reduction to N_2 (generalized here as "denitrification") in sediments and in suboxic zones of the water column (2). Given this biologically determined input/output budget, the variation or constancy of the oceanic fixed N reservoir has broader implications for the potential of ocean life to regulate environmental conditions on a global scale. Because the "major nutrients" N and phosphorus (P) fuel the biological sequestration of CO_2 in the deep ocean, changes in the oceanic fixed N reservoir have also been proposed as a driver of glacial/interglacial CO_2 change (3, 4).

Sediment records show N isotopic evidence of reduced water column denitrification during the Last Glacial Maximum (LGM) and other cold phases of the glacial cycles relative to the current interglacial (the "Holocene") and past warm time intervals (5, 6). "Benthic" denitrification (that which occurs in seafloor sediments) is equally as or more important than water column denitrification in the removal of N from the global ocean, and it has been hypothesized to decrease during glacials (times of high land ice volume) as well (7). This hypothesis is based on the generally rapid rate of denitrification in continental shelf sediments and on calculations that indicate the importance of shelf denitrification in the global ocean rate of denitrification (8). The continental shelves are characterized by high fluxes of organic matter to the sediments both because their shallow depth allows sinking matter to reach the bottom quickly and because the breakdown of organic matter in the shallow sediments returns nutrients immediately to the sunlit upper ocean. As a result, the nutrients supplied to the waters overlying the continental shelf drive multiple rapid cycles of productivity, sedimentation, and remineralization over its broad extent of shallow seafloor. During glacial maxima, the ∼120-m decline in sea level converted the continental shelves into coastal land, removing much of this environment as a site of oceanic N loss. The greater mean depth and steepness of the seaward continental slope should render the slope far less efficient at returning the nutrients released from the sediments to the upper ocean. Thus, upon sea level lowering, the coastal environment would be less favorable as an environment for both coastal productivity and benthic N loss. However, because the direct impact of benthic N loss on the N isotopes is typically nil or very weak (9, 10), there have been, as yet, no direct tests of this hypothesis.

Since the first studies of the ocean N budget, it has been recognized that a balance is required between inputs (dominantly N_2

Significance

Biologically available nitrogen (fixed N) limits the fertility of much of the ocean. Of the processes that remove fixed N from the ocean, conversion to N_2 in coastal sediments appears to dominate. This work provides the strongest data-based support for the long-standing hypothesis of changes in N loss along the ocean margin due to the cyclic drowning and emergence of the continental shelves. The data also imply strong local coupling of N loss to N_2 fixation, the dominant N input to the ocean, thus suggesting a stable oceanic fixed N reservoir over glacial cycles. Finally, this work points to glacial/interglacial oscillations in the biogeochemical fluxes at and near the ocean margins that would have influenced the evolution of coastal species.

Author contributions: H.R. and D.M.S. designed research; H.R. and M.S. performed research; H.R., R.F.A., M.-T.C., A.C.R., G.T.F.W., and G.H.H. contributed new reagents/analytic tools; H.R. and A.M.-G. analyzed data; and H.R. and D.M.S. wrote the paper.

The authors declare no conflict of interest.

This article is a PNAS Direct Submission.

Data deposition: The data reported in this work have been deposited with National Centers for Environmental Information (NOAA), https://www.ncdc.noaa.gov (accession no. 22390).

[1]To whom correspondence should be addressed. Email: abbyren@ntu.edu.tw.

This article contains supporting information online at www.pnas.org/lookup/suppl/doi:10.1073/pnas.1701315114/-/DCSupplemental.

fixation) and losses (dominantly denitrification) on the timescale of the residence time of fixed N in the ocean [currently ~3,000 y (2)], such that changes in N_2 fixation should be coupled to, and thus provide evidence of, changes in denitrification. It has been argued that denitrification generates a selective advantage to N_2 fixers by increasing the occurrence of phosphorus-bearing, N-depleted surface waters (i.e., excess phosphorus) (11). The resulting N_2 fixation response may thus yield spatial and temporal coupling between denitrification and N_2 fixation that balances the ocean's N budget, for which there are multiple lines of evidence (12–14). However, it has been pointed out that N_2 fixers have other sensitivities as well. In particular, both iron availability and temperature may be important constraints on N_2 fixation (3, 15).

The South China Sea (SCS) repeats end of paragraph is a marginal sea characterized by a high ratio of shelf area to basin area (~1.2). Deep SCS water has oceanographic characteristics similar to the western Pacific open ocean (16), with continuous exchange with the open western Pacific mainly through the Luzon Strait, which is ~2,200 m deep, too deep for the exchange of thermocline and deeper water masses to have been affected by glacial/interglacial sea level change. The warm tropical surface waters of the SCS and the adjacent Asian dust sources and ocean margins appear to leave N_2 fixation unconstrained by temperature or iron (17). The extensive East Asian and Sunda shelves host rapid sedimentary denitrification (8), which effectively removes fixed N and lowers the fixed nitrogen-to-phosphorus ratio (N/P) of the shallow water column in the region. These features suggest that the SCS may be prone to coupling between benthic denitrification and N_2 fixation.

The nitrogen isotopes can be used to reconstruct past changes in N_2 fixation in environments where the nitrogen isotopic signature of N_2 fixation can be clearly observed in the thermocline. N_2 fixation introduces N with a $\delta^{15}N$ of ~−1‰ versus atmospheric N_2 (18), which is distinctly lower than the $\delta^{15}N$ of oceanic nitrate (Fig. 1*B*). Mean ocean nitrate $\delta^{15}N$ is elevated above that of the newly fixed N (9) because water column denitrification removes nitrate (NO_3^-) that is depleted in ^{15}N (19). As a result, the remineralization of newly fixed N to nitrate causes regional lowering of nitrate $\delta^{15}N$ underneath the surface waters in which N_2 fixation occurs. This lowering is most intense in the shallow thermocline for two reasons. First, organic N is remineralized rapidly as it sinks, causing most of the sinking N and its isotopic signal of N_2 fixation to be emplaced at shallow depths. Second, nitrate concentration decreases upward across the thermocline, helping the nitrate that derives from local or regional N_2 fixation to represent a greater proportion of the total nitrate in the water. The lowering of nitrate $\delta^{15}N$ by N_2 fixation is perhaps most obvious today in the tropical and subtropical North Atlantic (20). However, a nitrate $\delta^{15}N$ minimum in the shallow thermocline is also observed in the North Pacific (21), including the SCS (22) (Fig. 1*C*).

The upward decline in nitrate $\delta^{15}N$ in the SCS thermocline is not observed everywhere in the tropical and subtropical North Pacific; for example, it is not observed in the equatorial or subarctic North Pacific (23, 24). Thus, it must be a reflection of N_2 fixation occurring in the western tropical/subtropical North Pacific. The shallow thermocline (i.e., the depth range of 100 m to 200 m) of the modern SCS has a much higher nitrate concentration (10 μM to 15 μM) than the same water depth or density level in the open subtropical North Pacific (<5 μM; Fig. 1*B* and Fig. S1). As a result, lateral exchange of the upper 200 m of the water column with the open western North Pacific has minimal capacity to change the $\delta^{15}N$ of nitrate in this depth

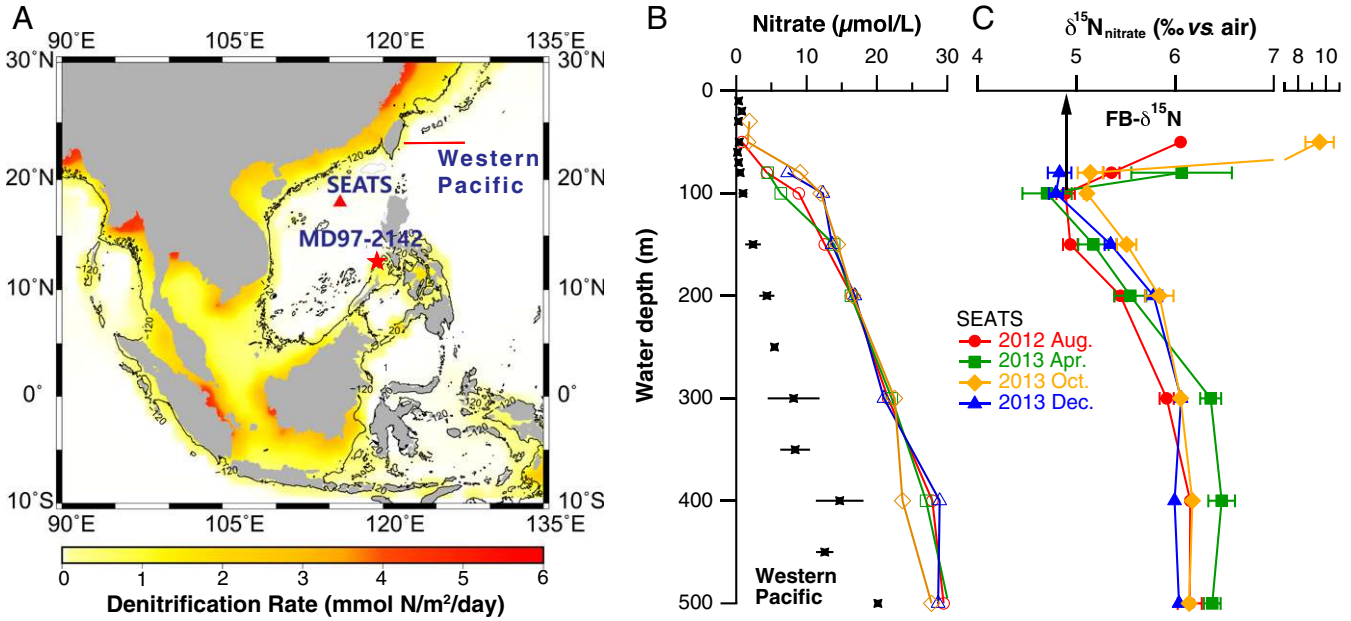

Fig. 1. Core location and modern context for this study. (*A*) Topographic map showing the change in basin configuration around the SCS between interglacial sea level high stand and full glacial sea level low stand, assuming a 120-m lowering of the shore line on modern topography (63) (black contour; modern land area shown in gray). The locations of the coring site for core MD97-2142, the SEATS, and the hydrographic transect in the open western Pacific are shown with a star, triangle, and line, respectively. Colors depict model-simulated benthic denitrification rate (millimoles of N per square meter per day) (8). The 120-m ice age sea level lowering exposes almost all of the shallow shelf where benthic denitrification is rapid in the present day. (*B* and *C*) The depth profiles of the concentration and $\delta^{15}N$ of nitrate plus nitrite in the upper 500 m at SEATS. The samples are collected from four cruises from 2012 summer to 2013 winter (indicated with different colors and symbols). The error bar at each depth indicates 1 SD associated with water collections from multiple casts during each cruise. The depth profile of the nitrate plus nitrite concentration in the open western Pacific is also shown for comparison (black squares). The remineralization of newly fixed N is taken as the dominant contributor to the subsurface nitrate $\delta^{15}N$ minimum and also lowers the nitrate $\delta^{15}N$ throughout the water column (22). The FB-$\delta^{15}N$ of both *G. ruber* and *O. universa* measured at the surface sediment are 4.9‰ (black arrow), similar to the $\delta^{15}N$ of the shallow thermocline nitrate being supplied to the photic zone.

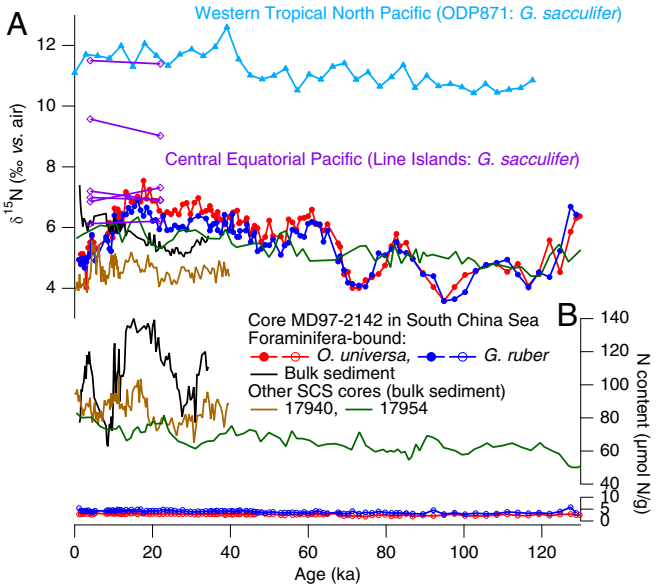

Fig. 2. Compilation of the (*A*) $\delta^{15}N$ and (*B*) N content of foraminifera-bound N and bulk sedimentary N records in the SCS and open Pacific. In SCS core MD97-2142, FB-$\delta^{15}N$ (filled circles) and N content (open circles) are shown for the planktonic foraminifera species *O. universa* (red circles) and *G. ruber* (blue circles) and for bulk sedimentary N (black line). Previously published bulk sedimentary $\delta^{15}N$ and N content from SCS cores 17940 and 17954 are also shown (green and brown lines) (27, 28). One open Pacific data set is a last ice age/Holocene FB-$\delta^{15}N$ comparison in cores from along the Line Islands in the central equatorial Pacific (purple diamonds) (36). The latitudes of the five cores are 0.22°S, 1.27°N, 2.46°N, 2.97°N, 5.2°N, and 6.83°N. Each core corresponds to paired LGM and Holocene data, with the FB-$\delta^{15}N$ from both the LGM and the Holocene increasing northward from the equator; from the assemblage of cores, no LGM-to-Holocene difference is observed. A second open Pacific data set is a record of FB-$\delta^{15}N$ from the western tropical north Pacific [ODP Site 871 (5.56°N, 172.35°E); blue triangles]. This record shows no clear FB-$\delta^{15}N$ decrease from the last ice age to the Holocene, in contrast to SCS FB-$\delta^{15}N$. The locations of the sediment cores are shown in Fig. S9.

range of the SCS. Therefore, the upward decline in nitrate $\delta^{15}N$ observed in the SCS thermocline (Fig. 1*C*) is probably mostly generated within the SCS.

Nitrate from the shallow thermocline supplied by vertical mixing is the dominant N source to the tropical and subtropical surface ocean on an annual basis (25). Thus, the $\delta^{15}N$ of the shallow thermocline nitrate is the dominant control on the $\delta^{15}N$ of net biomass production in the surface ocean each year, which, in turn, sets the $\delta^{15}N$ of the various species of planktonic foraminifera, the shells of which can be analyzed for the $\delta^{15}N$ of their fossil-bound organic N (26). As a consequence, foraminifera-bound N has a lower $\delta^{15}N$ in the modern SCS than in, for example, most of the equatorial Pacific (Fig. 2). Moreover, a higher rate of N_2 fixation in the SCS would cause a further decline in foraminifera-bound $\delta^{15}N$ (FB-$\delta^{15}N$), whereas slower N_2 fixation would cause a $\delta^{15}N$ rise.

Results and Discussion

Here we report a record of FB-$\delta^{15}N$ in the SCS over the last 860 ky, covering eight major glacial cycles (*Methods*). The sediment core is from site MD97-2142 on the slope off Palawan Island (Fig. 1*A*, 12°41′N, 119°27′E, water depth of 1,557 m, sedimentation rate of 10 cm/ky, age model shown in Fig. S2). The full record uses a single planktonic species, *Orbulina universa*. To test the generality of the *O. universa* FB-$\delta^{15}N$ record, the FB-$\delta^{15}N$ of *Globigerinoides ruber* was also analyzed over the last glacial cycle (back to ~125 ka). FB-$\delta^{15}N$ is expected to be similar for these two euphotic zone-dwelling species (26), and the data fit this expectation (Figs. 2 and 3). Slightly lower $\delta^{15}N$ is observed for *G. ruber* than for *O. universa* during the last ice age, with an average offset of 0.39‰ for 20 ka to 60 ka compared with 0.25‰ for the entire overlapping period (Fig. 2). The same sense of divergence (with the $\delta^{15}N$ of *O. universa* greater than that of *G. ruber*) is also observed in LGM samples from the Caribbean Sea (13), where it was tentatively interpreted to provide secondary support of the idea of reduced N_2 fixation during the LGM (13); a similar explanation may apply in the SCS. In any case, the changes in interspecies FB-$\delta^{15}N$ difference are minor relative to the FB-$\delta^{15}N$ changes shared by the two species.

The FB-$\delta^{15}N$ records have no clear correspondence with the bulk sediment records from the SCS, which do not show systematic glacial/interglacial changes (Fig. 2). Several of the existing bulk sediment records from the SCS are substantially dissimilar from one another (Fig. 2*A*) (27). Moreover, although foraminifera-bound N content is low and stable over glacial cycles, bulk sediment N content varies substantially over time and across records (Fig. 2*B*). Similar observations regarding SCS bulk sedimentary N records have previously been attributed to diagenesis and to multiple sources of N to the bulk sediment (28). Variation in terrigenous input at our study site has been documented to be associated with sea level change over the glacial cycles, for example, with higher concentrations of *n*-alkanes coinciding with lower sea level (29). A general disconnect between FB-$\delta^{15}N$ and bulk sediment $\delta^{15}N$ has been observed in the Caribbean Sea as well, where sedimentological data also point to terrestrial/shelf N inputs to the bulk sediments, especially in glacial intervals (13, 14). These findings argue against the utility

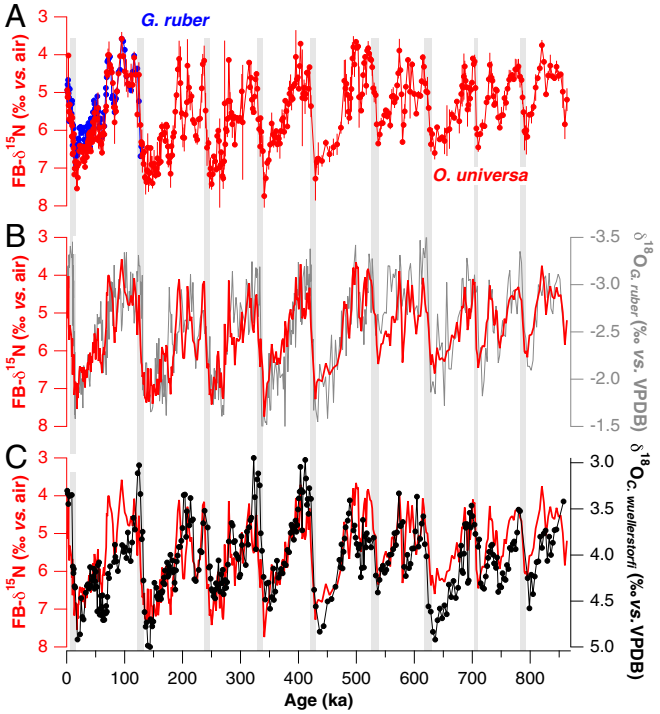

Fig. 3. Records of planktonic FB-$\delta^{15}N$ and planktonic and benthic foraminiferal calcite $\delta^{18}O$ over the last eight glacial cycles. FB-$\delta^{15}N$ is plotted decreasing upward, such that N_2 fixation increases upward. FB-$\delta^{15}N$ of *O. universa* (*A*–*C*, red) at MD97-2142 is similar to the FB-$\delta^{15}N$ of *G. ruber* (*A*, blue) during the last 130 ky. Error bars indicate 1 SD of the oxidation replicates (*Methods*). FB-$\delta^{15}N$ is highly correlated with the $\delta^{18}O$ of *G. ruber* (*B*, gray) (64) and of *C. wuellerstorfi* (*C*, black). The glacial/interglacial change in the $\delta^{18}O$ of the benthic foraminifera *C. wuellerstorfi* is typically considered to be mostly due to change in global ice volume (and hence sea level), with deep-water temperature change having a smaller effect. The light gray bars indicate the glacial terminations.

of bulk sediment $\delta^{15}N$ records for reconstructing the $\delta^{15}N$ of export production in marine environments such as the SCS and Caribbean Sea, where terrestrial and shelf inputs are significant, export production is modest, and sedimentary organic matter preservation is not exceptionally high.

The FB-$\delta^{15}N$ record from MD97-2142 indicates an increase in the $\delta^{15}N$ of subsurface nitrate of the SCS during the glacials (Fig. 3). Throughout the ocean, the $\delta^{15}N$ of subsurface nitrate is affected by lateral communication with other regions. Accordingly, one might propose that Pacific-wide processes raised the $\delta^{15}N$ of the nitrate in the SCS by ~3‰ during glacials. This might be driven by a whole ocean nitrate $\delta^{15}N$ rise. Alternatively, it might be driven by a change in the rate of circulation in and out of the SCS and/or a change in N-cycle processes outside the SCS.

With regard to changes in lateral circulation, as described above, there is no clear mechanism by which communication with open western North Pacific waters shallower than ~200 m could have a strong influence on SCS nitrate $\delta^{15}N$. Accordingly, this scenario must involve waters deeper than ~200 m. However, modern oceanic nitrate isotope data do not indicate that a change in lateral circulation by itself would significantly change intermediate-depth nitrate $\delta^{15}N$ in the SCS. For the western expanse of subtropical, subpolar, and tropical Pacific, even when including the western equatorial Pacific and existing measurements from the central South Pacific, the $\delta^{15}N$ of nitrate in intermediate-depth waters falls between 5.5‰ and 7.0‰, with most measurements in a still narrower range (23, 24, 30–35). Intermediate-depth nitrate in the modern SCS falls squarely in this range (Fig. 1 and Fig. S1), in part because of the rapid lateral exchange of the SCS with the neighboring open western North Pacific through the Luzon Strait. If this weak variation in intermediate-depth nitrate $\delta^{15}N$ also applied in the past, even major changes in the circulation of intermediate or mode waters would have had only modest effects on the $\delta^{15}N$ of the nitrate imported into the SCS.

We next consider the possibility of global and/or Pacific-wide changes in nitrate $\delta^{15}N$ that are communicated into the SCS. To compare with our record, we generated a 120-ky FB-$\delta^{15}N$ record using *Globigerinoides sacculifer* from western tropical North Pacific ([Ocean Drilling Program (ODP) 807]. This new record as well as paired LGM and Holocene FB-$\delta^{15}N$ data from the central equatorial Pacific (36) show only small $\delta^{15}N$ differences between the LGM and the Holocene (Fig. 2). Bulk sediment records from the eastern Pacific show the opposite sense of $\delta^{15}N$ change compared with that in the SCS (Fig. 4) (5, 37, 38). These and other records from across the global ocean argue against the possibility that the elevated FB-$\delta^{15}N$ observed in the SCS during the LGM reflects a change in the $\delta^{15}N$ of subsurface nitrate imported laterally from the open Pacific.

One might hypothesize greater vertical mixing in the SCS during ice ages, which might weaken the $\delta^{15}N$ decline upward through the SCS thermocline, thus increasing the $\delta^{15}N$ of the nitrate supply to the euphotic zone. However, this mechanism would predict simultaneous changes in productivity and FB-$\delta^{15}N$ in the oligotrophic SCS, and yet the productivity proxies are not particularly well correlated with FB-$\delta^{15}N$ (Fig. S3). Moreover, because deep thermocline waters have a substantially lower N/P ratio than the shallow thermocline waters (16), an increase in the supply of deeper-held nutrients to the surface would have encouraged an increase in N_2 fixation, which would have worked to lower the $\delta^{15}N$ of the sinking flux and of the shallow subsurface nitrate. This increase in N_2 fixation would have countered the tendency for increased vertical mixing to raise the $\delta^{15}N$ of the nitrate supply and, in turn, FB-$\delta^{15}N$. Finally, if changes in vertical mixing were the dominant driver of the $\delta^{15}N$ changes, we would expect synchronous changes in the sea surface temperature (SST) and $\delta^{15}N$, which is not supported by our data (Figs. 3, 4, and 5*A*). Similarly, it is observed that a planktonic foraminiferal index of vertical mixing (39) changes early in the deglaciation and then

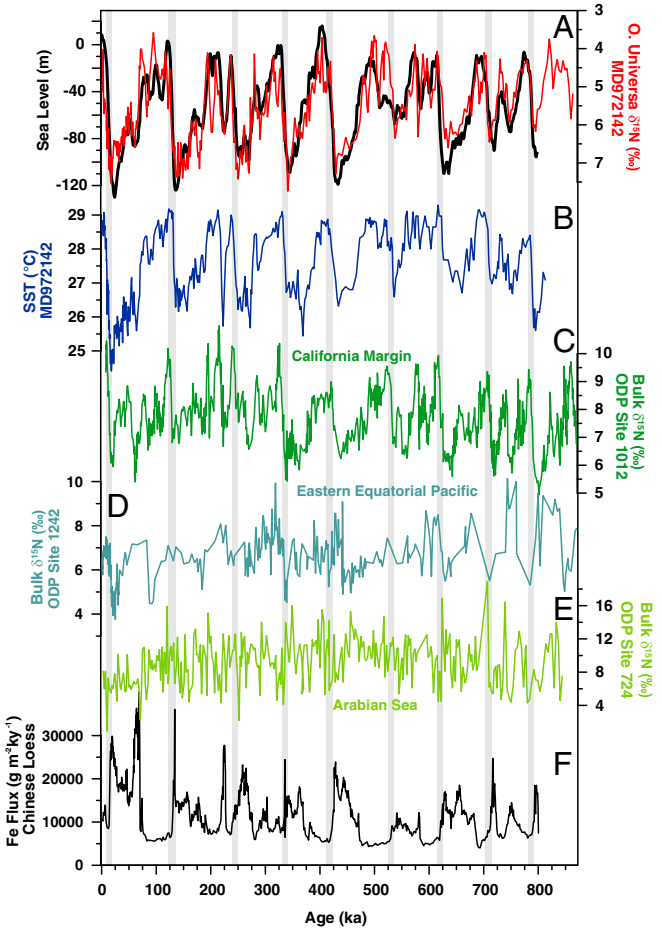

Fig. 4. Records of N_2 fixation, sea level, sea surface temperature, water column denitrification, and atmospheric iron supply. (*A*) Within the SCS, N_2 fixation is generally higher (FB-$\delta^{15}N$ is lower) in the interglacials (red; FB-$\delta^{15}N$ increases downward). N_2 fixation increases upon each termination and is tightly correlated with the mean relative sea level stack (black) generated using seven independent sea level reconstructions (49). (*B*) The structure of N_2 fixation variability is also similar to changes in sea surface temperature at MD97-2142 (29) but lags behind temperature changes, especially during the latter half of the record. Among the three records sensitive to water column denitrification from (*C*) the California margin (37), (*D*) eastern Equatorial Pacific (65), and (*E*) Arabian Sea (66), the bulk $\delta^{15}N$ record from the California margin is (negatively) correlated with FB-$\delta^{15}N$ in the SCS (note reversal of $\delta^{15}N$ scales between *A* and *C*–*E*). (*F*) A Chinese loess record shows generally higher iron flux in the glacials (67), which would increase N_2 fixation during glacials if iron availability were the primary control for N_2 fixation, inconsistent with the FB-$\delta^{15}N$ data. The light gray bars indicate the glacial terminations.

stabilizes, whereas FB-$\delta^{15}N$ evolves through the deglaciation and Holocene (Fig. 2) (40). As the effect of vertical exchange on nitrate $\delta^{15}N$ would be essentially instantaneous (decadal at most), this lag argues against SCS hydrographic conditions as the dominant signal in FB-$\delta^{15}N$.

Nitrogen inputs from river and atmospheric sources are also unlikely to explain the FB-$\delta^{15}N$ variations. Clear signs of riverine N input are confined to the inner shelf above 30 m, and our preliminary data from two summer cruises show high $\delta^{15}N$ values for the shallow shelf nitrate (up to 12‰). Atmospheric N deposition is low in $\delta^{15}N$ relative to oceanic nitrate (41), so an increase in deposition would have been required during interglacials to explain the low FB-$\delta^{15}N$. However, the interglacial $\delta^{15}N$ impact, when neglecting the recent rise in anthropogenic N, is far too low for its removal to have caused a 3‰ rise in FB-$\delta^{15}N$ during ice ages (42, 43).

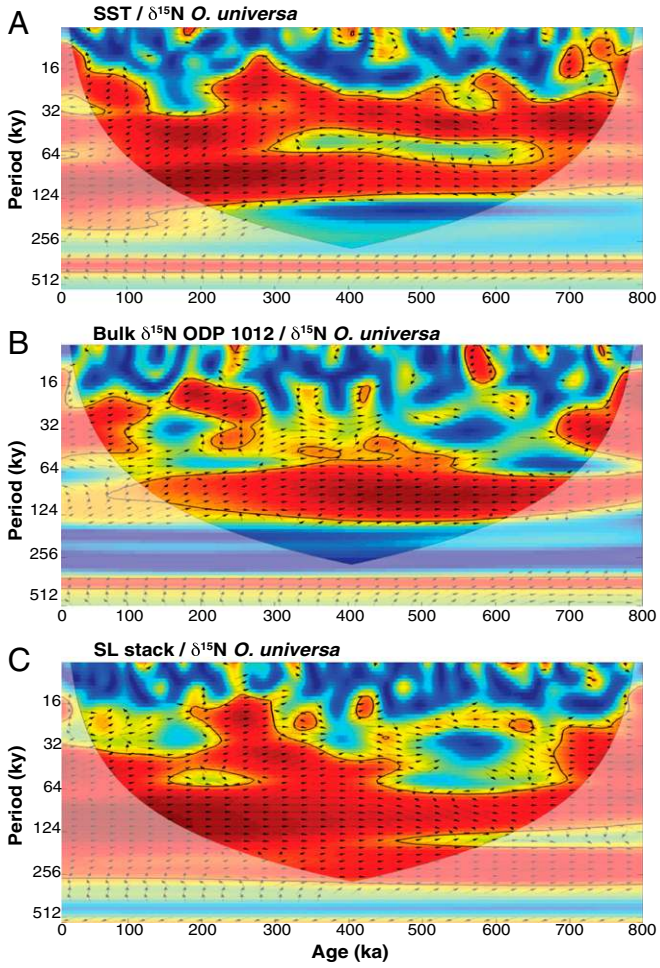

Fig. 5. Cross-wavelet coherence and phase relationship among records of N_2 fixation, sea level, sea surface temperature, and water column denitrification. Squared wavelet coherence between two time series was computed using the methods of ref. 68. The 95% confidence level against red noise was calculated using the Monte Carlo method and is shown as a thick contour that encloses the significant sections. The light shading indicates the region possibly influenced by edge effects. Black arrows indicate the phase relationship between the two time series, with in-phase pointing right, FB-δ^{15}N leading a given climate variable pointing down, and FB-δ^{15}N lagging pointing up. The different records have been interpolated to an evenly spaced time series of 2 ky before the spectral analysis. (*A*) The SST record (29) from the same sediment core has high coherency with, but leads, the FB-δ^{15}N of *O. universa* by around 4 ky during the last 400 ky at the dominant 41- and 100-ky bands, as indicated by the direction of the arrows, which is inconsistent with a causal connection in this case. (*B*) The bulk δ^{15}N record from California margin (37) is coherent with FB-δ^{15}N in the SCS at the period near 100 ky. (*C*) The sea level record stack (47–49) shows high coherency with FB-δ^{15}N at a wide range of frequencies.

A changing rate of N_2 fixation is the sole remaining mechanism with the potential to explain the cycles in FB-δ^{15}N at this site in the SCS. We conclude that the δ^{15}N of the shallow thermocline nitrate was lowered less by N_2 fixation during glacials, due to an ice age reduction in the rate of this process. The amplitude of the SCS δ^{15}N rise in the glacials is similar to that observed in the tropical western North Atlantic (13, 14), where N_2 fixation also has a strong imprint on thermocline nitrate δ^{15}N (20). The 3‰ amplitude of the glacial/interglacial FB-δ^{15}N change in the SCS is comparable to the largest regional declines in ocean nitrate δ^{15}N attributed to N_2 fixation in the modern ocean (44, 45); this suggests that the ice age decline in N_2 fixation rate was dramatic, most likely to less than half of the modern rate based on a two end-member mixing calculation (*Estimate for Glacial–Interglacial Changes in N_2 Fixation Rate*).

A question that arises is how FB-δ^{15}N glacial–interglacial variations of ∼3‰ could result when the modern nitrate δ^{15}N decline from ∼500 m depth into the shallow SCS thermocline is only 1 to 2‰ (Fig. 1*B*). First, the Holocene does not represent the minimum observed FB-δ^{15}N, so shallow thermocline nitrate δ^{15}N is reconstructed to have been still lower during previous interglacials. Second, the role of N_2 fixation in lowering the δ^{15}N of subsurface nitrate is greater than indicated by the local vertical gradient in nitrate δ^{15}N alone, as low δ^{15}N N from N_2 fixation spreads horizontally and vertically, as nitrate and sinking particulate nitrogen (45). This latter point also reinforces the arguments above against a hydrographic (e.g., vertical mixing) explanation for the observed FB-δ^{15}N changes.

At all nine glacial terminations covered by our FB-δ^{15}N record, a reconstructed increase in N_2 fixation in the SCS coincides with decreases in planktonic and benthic $\delta^{18}O_c$, a rise in sea level and thus an increase in shelf area (Fig. 4 and Figs. S4 and S5), a rise in SST, and an apparent deglacial increase in water column denitrification in the eastern tropical Pacific (Figs. 3 and 4). The length of the SCS FB-δ^{15}N record allows for the use of time series analysis to identify the correlations that are most consistent with a causal connection.

Variability in SST is highly coherent with that in FB-δ^{15}N (Fig. 5*A*). However, FB-δ^{15}N lags SST by more than 4 ky in the dominant 41- and 100-ky bands for the latter half of the record (Fig. 5*A*). Because the physiological and biochemical response of N_2 fixers to SST would be effectively instantaneous, the lag argues against SST as the driver of the greatest FB-δ^{15}N variations. Moreover, based on observed sensitivities (15), the reconstructed SCS SSTs fall into the optimal range for N_2 fixation, and a 3 °C cooling would be far too small to explain the dramatic reduction in N_2 fixation during glacials. Dust fluxes are lowest when reconstructed N_2 fixation is highest, arguing against iron supply as the explanation for the reconstructed N_2 fixation changes (Fig. 4*F*). This lack of positive correlation between N_2 fixation and dust supply is consistent with high iron availability in the SCS even during interglacials, both from the margins and from atmospheric deposition.

There are three bulk sediment δ^{15}N records from near water column zones of suboxia and that are adequately long to compare with our SCS FB-δ^{15}N record (Figs. 4 *C*–*E* and 5*B*). These environments are characterized by high export production and relatively good preservation of sedimentary organic matter, such that the potential of bulk sediment δ^{15}N to robustly record the δ^{15}N of N export is greater than in most other ocean regions (46). Of these records, only ODP Site 1012 (37) from the California margin shows significant coherency (Figs. 4*C* and 5*B*). The anticorrelation of the records might be taken to suggest that enhanced water column denitrification in the eastern tropical North Pacific during interglacials was responsible for coincident N_2 fixation in the SCS. However, the coherency is limited to periods near 100 ky, suggesting that observed similarities in the records reflect independent but similarly timed responses to glacial cycles.

The SCS FB-δ^{15}N and $\delta^{18}O_c$ records are similar in large-scale structure (Figs. 3 *B* and *C*), suggesting a connection between N_2 fixation and sea level. A stack of sea level records (47–49) shows high coherency with the SCS FB-δ^{15}N over a wide range of frequencies (Fig. 5*C*; significant against red noise with 95% confidence), as strong as the coherency between independent sea level reconstructions (Figs. S6–S8). Thus, the reconstructed glacial/interglacial changes in N_2 fixation appear to require a mechanism that involves ice volume and/or sea level change. The correlation of markers of terrigenous input with FB-δ^{15}N in MD972142, with greater terrigenous material when FB-δ^{15}N is high (29), provides additional support for this interpretation (Fig. S3*D*). As no relatively direct, low-lag connection between ice volume and N_2 fixation appears plausible for the SCS, the data argue for sea level as the dominant driver of N_2 fixation change.

The extensive continental shelf area of the tropical western North Pacific adjacent to the SCS, the Sunda shelf in particular, appears to be an important locus of benthic denitrification (8). This shelf area was nearly completely lost during peak glacials (Fig. 1*A*). The reduction in shelf area has been proposed to reduce shelf sedimentary denitrification in the glacials (7), which, in turn, would lead to higher N/P (less excess P) in the upper water column. This change would have discouraged N_2 fixation in the SCS and neighboring regions, explaining the remarkable coherency of the sea level records and our SCS FB-δ^{15}N record (Fig. 6).

The SCS FB-δ^{15}N record thus provides the most direct evidence to date for the long-hypothesized scenario in which sea level drives glacial cycles in benthic N loss along the continental margins. Such a mechanism implies that SCS N_2 fixation responded to changes in nearby shelf area, as changes in N loss on distant shelves should have been compensated by N_2 fixation in those regions. N_2 fixation compensation for N loss might be confounded by changes in iron availability in other tropical/subtropical ocean regions. However, for regions such as the SCS that are characterized by high iron supply, local compensation for N loss changes is arguably to be expected.

Continental slopes are known to deposit substantial quantities of margin-derived organic matter at their base (50), and the resulting accumulation drives denitrification on the slope (31, 51, 52). It is possible that this process was accelerated during ice ages and, in part, replaced the sedimentary denitrification on the continental shelves. N loss on the slope may not lead to synchronous changes in N_2 fixation because the N deficit would accumulate in deep water, not directly affecting the N/P of the nutrient supply to the locally overlying surface ocean. However, the funneling of organic matter into the deep ocean prevents the upper ocean nutrient recycling and other processes that render N loss so rapid on the shelves. Therefore, any increased N loss by denitrification on the slope is unlikely to have substantially compensated for the reduced N loss on the shallow margins.

N_2 fixation slowed substantially during ice ages, as reconstructed here for the western tropical Pacific and previously for the North Atlantic, in both cases consistent with the response of N_2 fixation to excess P supply as the dominant driver of the changes (13, 14). The correlation between SCS N_2 fixation and sea level provides data-based support for the hypothesis of reduced sedimentary denitrification during ice ages (7, 53, 54), and bulk sediment δ^{15}N records argue for reductions in water column denitrification as well (5, 6). With these lower rates of both input and loss, the residence time of fixed N in the ocean [currently ~3 ky (55, 56)] would have become longer and thus less distinct from the residence time of phosphorus [15 ky to 40 ky (57)], although the latter may also have changed over glacial cycles.

Benthic N loss on the continental margins reflects the high flux of organic matter to the coastal seabed (50–52), a consequence of both the shallow continental shelf and the high productivity of the coastal water column (Fig. 6). The high productivity is, in turn, supported by the shelf, which traps sinking organic matter and quickly returns nutrients to the sunlit surface ocean. Thus, the reduction in benthic N loss during ice ages implies a net decline in the organic matter supply to coastal ecosystems, especially those organisms that rely on the benthos. In part because of their extraordinarily high productivity and benthic activity, the modern continental shelves have tremendous importance for seafloor fauna, fish, and marine mammals. The reconstructed biogeochemical changes imply that these higher trophic levels would have suffered a notable decline in food supply during the low sea level stands of ice ages (Fig. 6), potentially impacting the evolution and current characteristics of coastal species and ecosystems (e.g., ref. 58).

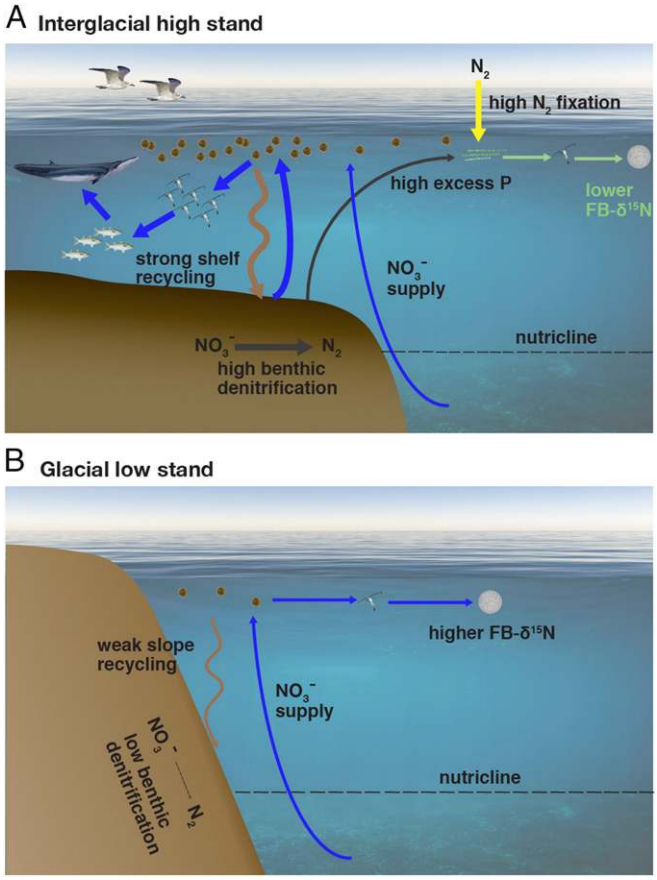

Fig. 6. Inferred glacial/interglacial changes along the SCS margin. (*A*) During interglacial high sea level stands, organic matter decomposition on the shallow shelf promotes high coastal ocean productivity and rapid shelf denitrification. The denitrification, by consuming fixed N, causes the shelf water to have excess P. When this water is transported into the open SCS, phytoplankton growth draws down its nutrients, and its excess P causes N to become depleted before P. The availability of P in the absence of N enhances N_2 fixation, which is reflected in a lowering of thermocline nitrate δ^{15}N and thus lower FB-δ^{15}N. (*B*) The sea level-driven loss of the shallow shelf during glacials reduces productivity and sedimentary denitrification along the margin. The reduction in sedimentary denitrification rate is compensated by slower offshore N_2 fixation, causing thermocline nitrate δ^{15}N and FB-δ^{15}N to rise. Along the margin, the glacial reduction in shallow seafloor nutrient recycling and thus phytoplankton production would impact the upper trophic levels that thrive on the modern (interglacial) shelf. This mechanism, which explains the observed coupled changes in sea level and N_2 fixation in the SCS, should also apply along other ocean margins.

Methods

FB-δ^{15}N Analyses. The protocol follows and is modified from that of refs. 13 and 14. The individual foraminifera species (250- to 425-μm-size fraction, ~5 mg per sample) are picked manually and gently crushed under a dissecting microscope. Samples are first sonicated for 5 min in an ultrasonic bath using 2% polyphosphate solution to remove clay particles. To remove metal coatings, bicarbonate-buffered dithionite–citric acid solution is then added to each sample, and the samples are placed in a water bath at 80 °C for 1 h. The final cleaning step is oxidative: Basic potassium persulfate solution is added to each sample, and the samples are autoclaved (at 121 °C) for 1 h. The cleaned samples are rinsed in deionized water and dried overnight at 55 °C. This cleaning protocol typically preserves 60 to 75% of the initial foraminifera weight.

Cleaned foraminifera (~3 mg to 4 mg per sample) are weighed into a previously combusted glass vial and dissolved in 3N HCl. To convert the released organic N to nitrate, purified basic potassium persulfate oxidizing solution is added to the vials, which are then autoclaved for 1 h on a slow-vent setting. To lower the N blank associated with the oxidizing solution, the potassium persulfate is recrystallized three times. At the time of processing, 0.8 g of NaOH and 0.5 g of potassium persulfate are dissolved in 100 mL of deionized water. Organic standards are used to constrain the δ^{15}N of the persulfate reagent blank. Three different organic standards were used: US Geological Survey (USGS) 40 (δ^{15}N = −4.5‰ vs. air), USGS 41 (δ^{15}N = 47.6‰ vs. air), and a laboratory standard made of a mixture of 6-aminocaproic acid

and glycine ($\delta^{15}N$ = 5.4‰ vs. air). A minimum of 18 organic standards and three to five blanks were analyzed per batch of samples.

To determine the N content of the samples, nitrate concentration is measured in the oxidation solution after autoclaving. The nitrate analysis is by reduction to nitric oxide using vanadium (III) followed by chemiluminescence detection (59). The blank is also quantified in this way. Consistent with our previous findings, *O. universa* and *G. ruber* had an average N content of 3 mmol to 4 mmol N per gram of cleaned calcite, yielding nitrate concentrations in the oxidation solutions of 10 μM to 20 μM, whereas the nitrate concentration of the blanks ranged between 0.3 μM and 0.7 μM (less than 5%, typically less than 2%, of the total N per sample).

The $\delta^{15}N$ of the samples is determined using the denitrifier method in conjunction with gas chromatography and isotope ratio mass spectrometry (60, 61). The denitrifier method involves the transformation of dissolved nitrate and nitrite into nitrous oxide gas (N_2O) via a naturally occurring denitrifying bacterial strain that lacks an active form of the enzyme N_2O reductase. Before adding the foraminifera samples to the bacteria, the sample solution is acidified to pH 3 to 7. The denitrifier *Pseudomonas chlororaphis* was used for this work. Normally, 5-nmol samples are added to 1.5 mL of bacterial concentrate after degassing of the bacteria. Along with the samples, the organic standards as well as replicate analyses of nitrate reference material International Atomic Energy Agency NO3 reference (IAEA-N3) ($\delta^{15}N$ = 4.7‰ vs. air) and a bacterial blank are also measured. The IAEA-N3 standards are used to monitor the bacterial conversion and the stability of the mass spectrometry, and the oxidation standards are used to correct for the oxidation blanks. If possible, samples were oxidized in duplicate, and oxidized samples were also sometimes analyzed by the denitrifier method in duplicate. The denitrifier method typically has a SD (1σ) of less than 0.1‰ and is not reported here. The reported error is the SD estimated from the means of separate oxidations of cleaned foraminiferal material, which averaged 0.22‰ (57% were less than 0.2‰, and 93% were less than 0.5‰).

The data reported in this work will be accessible at National Centers for Environmental Information (NOAA) once the paper is published online.

The $\delta^{18}O$ Analyses on *Cibicidoides wuellerstorfi*. Approximately 15 *Cibicidoides wuellerstorfi* individuals were picked from each sample. The samples were ultrasonicated first in 1 mL of deionized water for 3 s to 5 s, then in 0.2 mL of methanol for 3 s to 5 s. The samples were rinsed with deionized water two to three times and dried in an oven at 60 °C overnight. The cleaned foraminifera samples were crushed, and 35 mg to 80 mg weighed into 4.5-mL vials. The $\delta^{18}O$ were analyzed with a Thermo GasBench II coupled to a Thermo Delta V Plus mass spectrometer at Eidgenössische Technische Hochschule Zürich (62). The average of the SD of single $\delta^{18}O$ measurements is ∼0.04%.

Nitrate Sampling and $\delta^{15}N$ Analyses at the South East Asian Time-Series Station and in the Open Western Pacific. The South East Asian Time-Series (SEATS) station is located at 18°N and 116°E (Fig. 1*A*) in about 3,800 m of water. It was sampled four times between August 2012 and December 2013 in approximately seasonal intervals aboard R/V *Ocean Researcher I*. Two casts during August 2012 and eight casts from each of the other three cruises were sampled for nitrate $\delta^{15}N$ analyses. The western subtropical Pacific transect is located along 23.5°N from 122.25°E to 126°E. Discrete water samples were collected from five open ocean stations in 2013 July on R/V *Ocean Research V*. All water samples were collected with General Oceanics GO-FLO bottles bottles mounted onto a Rosette sampling assembly. From each depth, seawater was collected unfiltered in a rinsed 60-mL high-density polyethylene bottle and immediately frozen at −20 °C.

The concentration of nitrate plus nitrite was analyzed by reduction to nitric oxide using vanadium (III) followed by chemiluminescence detection (59). The $\delta^{15}N$ of nitrate was determined using the denitrifier method, as described above. We use two international nitrate isotope reference materials, IAEA-N3 ($\delta^{15}N$ = 4.7‰ vs. air) and USGS-34 ($\delta^{15}N$ = −1.8‰ vs. air), to correct the data. The analytical precision for $\delta^{15}N$ was 0.08‰. The error bars in Fig. 1*C* represent 1 SD of the nitrate $\delta^{15}N$ analyzed at the same depth from the different casts, which averaged 0.20‰.

ACKNOWLEDGMENTS. We thank M. A. Weigand and S. Oleynik for assistance with the nitrate and foraminifera-bound $\delta^{15}N$ analyses; Tung-Yuan Ho, Kuo-Yuan Lee, and Yao-Chu Wu for their assistance on cruises and water sampling; and M. P. Hain for discussions. Funding was provided by Taiwan Ministry of Science and Technology (MOST) Grant 105-2628-M-002-007-MY3, by National Taiwan University Grant NTU-CESRP-106R7625-1 (to H.R.), by MOST Grant NSC 101-2611-M-001-003-MY3 and a grant from the Sustainability Science Research Program of the Academia Sinica (to G.T.F.W.), by the US National Science Foundation through Grants OCE-1060947 and PLR-1401489 (to D.M.S.), and by the Grand Challenges Program of Princeton University.

1. Moore JK, Lindsay K, Doney SC, Long MC, Misumi K (2013) Marine ecosystem dynamics and biogeochemical cycling in the Community Earth System Model [CESM1(BGC)]: Comparison of the 1990s with the 2090s under the RCP4.5 and RCP8.5 Scenarios. *J Clim* 26:9291–9312.
2. Gruber N, Galloway JN (2008) An Earth-system perspective of the global nitrogen cycle. *Nature* 451:293–296.
3. Falkowski PG (1997) Evolution of the nitrogen cycle and its influence on the biological sequestration of CO_2 in the ocean. *Nature* 387:272–275.
4. Broecker WS, Henderson GM (1998) The sequence of events surrounding Termination II and their implications for the cause of glacial-interglacial CO_2 changes. *Paleoceanography* 13:352–364.
5. Ganeshram RS, Pedersen TF, Calvert SE, Murray JW (1995) Large changes in oceanic nutrient inventories from glacial to interglacial periods. *Nature* 376:755–758.
6. Altabet MA, Francois R, Murray DW, Prell WL (1995) Climate-related variations in denitrification in the Arabian Sea from sediment $^{15}N/^{14}N$ ratios. *Nature* 373:506–509.
7. Christensen JP (1994) Carbon export from continental shelves, denitrification and atmospheric carbon dioxide. *Cont Shelf Res* 14:547–576.
8. Bianchi D, Dunne JP, Sarmiento JL, Galbraith ED (2012) Data-based estimates of suboxia, denitrification, and N_2O production in the ocean and their sensitivities to dissolved O_2. *Glob Biogeochem Cycles* 26:GB2009.
9. Brandes JA, Devol AH (1997) Isotopic fractionation of oxygen and nitrogen in coastal marine sediments. *Geochim Cosmochim Acta* 61:1793–1801.
10. Lehmann MF, Sigman DM, Berelson WM (2004) Coupling the N-15/N-14 and O-18/O-16 of nitrate as a constraint on benthic nitrogen cycling. *Mar Chem* 88:1–20.
11. Sañudo-Wilhelmy SA, et al. (2001) Phosphorus limitation of nitrogen fixation by *Trichodesmium* in the central Atlantic Ocean. *Nature* 411:66–69.
12. Deutsch C, Sarmiento JL, Sigman DM, Gruber N, Dunne JP (2007) Spatial coupling of nitrogen inputs and losses in the ocean. *Nature* 445:163–167.
13. Ren H, et al. (2009) Foraminiferal isotope evidence of reduced nitrogen fixation in the ice age Atlantic Ocean. *Science* 323:244–248.
14. Straub M, et al. (2013) Changes in North Atlantic nitrogen fixation controlled by ocean circulation. *Nature* 501:200–203.
15. Houlton BZ, Wang YP, Vitousek PM, Field CB (2008) A unifying framework for dinitrogen fixation in the terrestrial biosphere. *Nature* 454:327–330.
16. Wong GTF, Ku T-L, Mulholland M, Tseng C-M, Wang D-P (2007) The SouthEast Asian Time-series Study (SEATS) and the biogeochemistry of the South China Sea—An overview. *Deep Sea Res Part II Top Stud Oceanogr* 54:1434–1447.
17. Zhang R, et al. (2015) Physical-biological coupling of N_2 fixation in the northwestern South China Sea coastal upwelling during summer. *Limnol Oceanogr* 60:1411–1425.
18. Wada E, Terazaki M, Kabaya Y, Nemoto T (1987) ^{15}N and ^{13}C abundances in the Antartic Ocean with emphasis on the biogeochemical structure of the food web. *Deep Sea Res Part A Oceanogr Res Pap* 34:829–841.
19. Brandes JA, Devol AH, Yoshinari T, Jayakumar DA, Naqvi SWA (1998) Isotopic composition of nitrate in the central Arabian Sea and eastern tropical North Pacific: A tracer for mixing and nitrogen cycles. *Limnol Oceanogr* 43:1680–1689.
20. Knapp AN, DiFiore PJ, Deutsch C, Sigman DM, Lipschultz F (2008) Nitrate isotopic composition between Bermuda and Puerto Rico: Implications for N_2 fixation in the Atlantic Ocean. *Glob Biogeochem Cycles* 22:GB3014.
21. Liu KK, Su MJ, Hsueh CR, Gong GC (1996) The nitrogen isotopic composition of nitrate in the Kurosio Water northeast of Taiwan: Evidence for nitrogen fixation as a source of isotopically light nitrate. *Mar Chem* 54:273–292.
22. Wong GTF, et al. (2002) Nitrate anomaly in the upper nutricline in the northern South China Sea - Evidence for nitrogen fixation. *Geophys Res Lett* 29:2097.
23. Ren H, et al. (2015) Glacial-to-interglacial changes in nitrate supply and consumption in the subarctic North Pacific from microfossil-bound N isotopes at two trophic levels. *Paleoceanography* 30:1217–1232.
24. Rafter PA, Sigman DM, Charles CD, Kaiser J, Haug GH (2012) Subsurface tropical Pacific nitrogen isotopic composition of nitrate: Biogeochemical signals and their transport. *Glob Biogeochem Cycles* 26:GB1003.
25. Chavez EP, Toggweiler JR (1995) *Physical Estimates of Global New Production: The Upwelling Contribution* (Wiley, New York).
26. Ren H, Sigman DM, Thunell RC, Prokopenko MG (2012) Nitrogen isotopic composition of planktonic foraminifera from the modern ocean and recent sediments. *Limnol Oceanogr* 57:1011–1024.
27. Kienast M (2000) Unchanged nitrogen isotopic composition of organic matter in the South China Sea during the last climatic cycle: Global implications. *Paleoceanography* 15:244–253.
28. Kienast M, et al. (2005) On the sedimentological origin of down-core variations of bulk sedimentary nitrogen isotope ratios. *Paleoceanography* 20:PA2009.
29. Shiau LJ, et al. (2008) Sea surface temperature, productivity, and terrestrial flux variations of the southeastern South China Sea over the past 800000 years (IMAGES MD972142). *Terr Atmos Ocean Sci* 19:363–376.
30. Casciotti KL, Trull TW, Glover DM, Davies D (2008) Constraints on nitrogen cycling at the subtropical North Pacific Station ALOHA from isotopic measurements of nitrate and particulate nitrogen. *Deep Sea Res Part II Top Stud Oceanogr* 55:1661–1672.
31. Lehmann MF, et al. (2005) Origin of the deep Bering Sea nitrate deficit: Constraints from the nitrogen and oxygen isotopic composition of water column nitrate and benthic nitrate fluxes. *Glob Biogeochem Cycles* 19:GB4005.

32. Kienast M, et al. (2008) A mid-Holocene transition in the nitrogen dynamics of the western equatorial Pacific: Evidence of a deepening thermocline? *Geophys Res Lett* 35:L23610.
33. Rafter PA, Difiore PJ, Sigman DM (2013) Coupled nitrate nitrogen and oxygen isotopes and organic matter remineralization in the Southern and Pacific Oceans. *J Geophys Res Oceans* 118:4781–4794.
34. Rafter PA, Sigman DM (2015) Spatial distribution and temporal variation of nitrate nitrogen and oxygen isotopes in the upper equatorial Pacific Ocean. *Limnol Oceanogr* 61:14–31.
35. Sigman DM, DiFiore PJ, Hain MP, Deutsch C, Karl DM (2009) Sinking organic matter spreads the nitrogen isotope signal of pelagic denitrification in the North Pacific. *Geophys Res Lett* 36:L08605.
36. Costa KM, et al. (2016) No iron fertilization in the equatorial Pacific Ocean during the last ice age. *Nature* 529:519–522.
37. Liu Z, Altabet MA, Herbert TD (2008) Plio-Pleistocene denitrification in the eastern tropical North Pacific: Intensification at 2.1 Ma. *Geochem Geophys Geosyst* 9:Q11006.
38. Studer AS, Ellis KK, Oleynik S, Sigman DM, Haug GH (2013) Size-specific opal-bound nitrogen isotope measurements in North Pacific sediments. *Geochim Cosmochim Acta* 120:179–194.
39. Yu P-S, Huang C-C, Chin Y, Mii H-S, Chen M-T (2006) Late Quaternary East Asian Monsoon variability in the South China Sea: Evidence from planktonic foraminifera faunal and hydrographic gradient records. *Palaeogeogr Palaeoclimatol Palaeoecol* 236:74–90.
40. Ren H, Sigman DM, Chen M-T, Kao S-J (2012) Elevated foraminifera-bound nitrogen isotopic composition during the last ice age in the South China Sea and its global and regional implications. *Glob Biogeochem Cycles* 26:GB1031.
41. Yang JYT, Hsu SC, Dai M, Hsiao SSY, Kao SJ (2013) Isotopic composition of water-soluble nitrate in bulk atmospheric deposition at Dongsha Island: sources and implications of external N supply to the northern South China Sea. *Biogeosci Discuss* 10: 9661–9695.
42. Yang S, Gruber N (2016) The anthropogenic perturbation of the marine nitrogen cycle by atmospheric deposition: Nitrogen cycle feedbacks and the ^{15}N Haber-Bosch effect. *Glob Biogeochem Cycles* 30:1418–1440.
43. Ren H, et al. (2017) 21st-century rise in anthropogenic nitrogen deposition on a remote coral reef. *Science* 356:749–752.
44. Sigman DM, et al. (2009) The dual isotopes of deep nitrate as a constraint on the cycle and budget of oceanic fixed nitrogen. *Deep Sea Res Part I Oceanogr Res Pap* 56: 1419–1439.
45. Marconi D, et al. (2015) Nitrate isotope distributions on the US GEOTRACES North Atlantic cross-basin section: Signals of polar nitrate sources and low latitude nitrogen cycling. *Mar Chem* 177:143–156.
46. Altabet MA, et al. (1999) The nitrogen isotope biogeochemistry of sinking particles from the margin of the Eastern North Pacific. *Deep Sea Res Part I Oceanogr Res Pap* 46:655–679.
47. Elderfield H, et al. (2012) Evolution of ocean temperature and ice volume through the mid-Pleistocene climate transition. *Science* 337:704–709.
48. Bintanja R, van de Wal RS (2008) North American ice-sheet dynamics and the onset of 100,000-year glacial cycles. *Nature* 454:869–872.
49. Spratt RM, Lisiecki LE (2016) A Late Pleistocene sea level stack. *Clim Past* 12: 1079–1092.
50. Reimers CE, Jahnke RA, Mccorkle DC (1992) Carbon fluxes and burial rates over the continental slope and rise off central California with implications for the global carbon cycle. *Glob Biogeochem Cycles* 6:199–224.
51. Joye SB, Anderson IC (2008) Nitrogen cycling in coastal sediments. *Nitrogen in the Marine Environment*, eds Capone DG, Bronk DA, Mulholland MR, Carpenter EJ (Academic, San Diego), 2nd Ed, pp 867–915.
52. Devol AH (2015) Denitrification, anammox, and N_2 production in marine sediments. *Annu Rev Mar Sci* 7:403–423.
53. Galbraith ED, et al. (2013) The acceleration of oceanic denitrification during deglacial warming. *Nat Geosci* 6:579–584.
54. Deutsch C, Sigman DM, Thunell RC, Meckler AN, Haug GH (2004) Isotopic constraints on glacial/interglacial changes in the oceanic nitrogen budget. *Glob Biogeochem Cycles* 18:GB4012.
55. Brandes JA, Devol AH (2002) A global marine-fixed nitrogen isotopic budget: Implications for Holocene nitrogen cycling. *Glob Biogeochem Cycles* 16:1120.
56. Gruber N (2004) The dynamics of the marine nitrogen cycle and its influence on atmospheric CO_2 variations. *The Ocean Carbon Cycle and Climate*, NATO Science Series, eds Follows M, Oguz T, (Springer, Dordrecht, The Netherlands), Vol 40, pp 97–148.
57. Ruttenberg KC (1993) Reassessment of the oceanic residence time of phosphorus. *Chem Geol* 107:405–409.
58. Pyenson ND, Lindberg DR (2011) What happened to gray whales during the Pleistocene? The ecological impact of sea-level change on benthic feeding areas in the North Pacific Ocean. *PLoS One* 6:e21295.
59. Braman RS, Hendrix SA (1989) Nanogram nitrite and nitrate determination in environmental and biological materials by vanadium (III) reduction with chemiluminescence detection. *Anal Chem* 61:2715–2718.
60. Sigman DM, et al. (2001) A bacterial method for the nitrogen isotopic analysis of nitrate in seawater and freshwater. *Anal Chem* 73:4145–4153.
61. Casciotti KL, Sigman DM, Hastings MG, Böhlke JK, Hilkert A (2002) Measurement of the oxygen isotopic composition of nitrate in seawater and freshwater using the denitrifier method. *Anal Chem* 74:4905–4912.
62. Breitenbach SFM, Bernasconi SM (2011) Carbon and oxygen isotope analysis of small carbonate samples (20 to 100 μg) with a GasBench II preparation device. *Rapid Commun Mass Spectrom* 25:1910–1914.
63. Yokoyama Y, Lambeck K, De Deckker P, Johnston P, Fifield LK (2000) Timing of the Last Glacial Maximum from observed sea-level minima. *Nature* 406:713–716.
64. Wei K-Y, Chiu T-C, Chen Y-G (2003) Toward establishing a maritime proxy record of the East Asian summer monsoons for the late Quaternary. *Mar Geol* 201:67–79.
65. Robinson RS, Etourneau J, Martinez PM, Schneider R (2014) Expansion of pelagic denitrification during early Pleistocene cooling. *Earth Planet Sci Lett* 389:52–61.
66. Higginson MJ, Altabet MA, Murray DW, Murray RW, Herbert TD (2004) Geochemical evidence for abrupt changes in relative strength of the Arabian monsoons during a stadial/interstadial climate transition. *Geochim Cosmochim Acta* 68:3807–3826.
67. Guo ZT, Berger A, Yin QZ, Qin L (2009) Strong asymmetry of hemispheric climates during MIS-13 inferred from correlating China loess and Antarctica ice records. *Clim Past* 5:21–31.
68. Grinsted A, Moore JC, Jevrejeva S (2004) Application of the cross wavelet transform and wavelet coherence to geophysical time series. *Nonlinear Process Geophys* 11: 561–566.
69. Hoering TC, Ford HT (1960) The isotope effect in the fixation of nitrogen by azotobacter. *J Am Chem Soc* 82:376–378.
70. Minagawa M, Wada E (1986) Nitrogen isotope ratios of red tide organisms in the East China Sea: A characterization of biological nitrogen fixation. *Mar Chem* 19:245–259.
71. Carpenter EJ, Harvey HR, Fry B, Capone DG (1997) Biogeochemical tracers of the marine cyanobacterium *Trichodesmium*. *Deep Sea Res Part I Oceanogr Res Pap* 44: 27–38.
72. Broecker WS, Patzert WC, Toggweiler JR, Stuiver M (1986) Hydrography, chemistry, and radioisotopes in the Southeast Asian basins. *J Geophys Res Oceans* 91:2156–2202.
73. Amante C, Eakins BW (2009) *ETOPO1 1 Arc-Minute Global Relief Model: Procedures, Data Sources and Analysis* (Natl Geophys Data Cent, Boulder, CO), NOAA Tech Memo NESDIS NGDC-24.
74. Lisiecki LE, Raymo ME (2005) A Pliocene-Pleistocene stack of 57 globally distributed benthic $\delta^{18}O$ records. *Paleoceanography* 20:PA1003.
75. Shakun JD, Lea DW, Lisiecki LE, Raymo ME (2015) An 800-kyr record of global surface ocean $\delta^{18}O$ and implications for ice volume-temperature coupling. *Earth Planet Sci Lett* 426:58–68.
76. Rohling EJ, et al. (2014) Sea-level and deep-sea-temperature variability over the past 5.3 million years. *Nature* 508:477–482.
77. Sosdian S, Rosenthal Y (2009) Deep-sea temperature and ice volume changes across the Pliocene-Pleistocene climate transitions. *Science* 325:306–310.